

西天山达巴特 A 型花岗岩的形成时代与构造背景^{*}

唐功建^{1,2} 陈海红³ 王强^{1**} 赵振华¹ Derek A. Wyman⁴ 姜子琦^{1,2} 贾小辉^{1,2}

TANG GongJian^{1,2}, CHEN HaiHong³, WANG Qiang^{1**}, ZHAO ZhenHua¹, Derek A. Wyman⁴, JIANG ZiQi^{1,2} and JIA XiaoHui^{1,2}

1. 中国科学院广州地球化学研究所同位素年代学与地球化学重点实验室, 广州 510640

2. 中国科学院研究生院, 北京 100049

3. 中国地质大学(武汉)地质过程与矿产资源国家重点实验室, 武汉 4300474

4. 悉尼大学地球科学学院地质与地球物理系, 新南威尔士 2006, 澳大利亚

1. Key Laboratory of Isotope Geochronology and Geochemistry, Guangzhou Institute of Geochemistry, Chinese Academy of Sciences, Guangzhou 510640, China

2. Graduate University of Chinese Academy of Sciences, Beijing 100049, China

3. State Key Laboratory of Geological Processes and Mineral Resources, China University of Geosciences, Wuhan 430074, China

4. Division of Geology and Geophysics, School of Geosciences, The University of Sydney, NSW 2006, Australia

2008-01-12 收稿, 2008-05-06 改回.

Tang GJ, Chen HH, Wang Q, Zhao ZH, Wyman DA, Jiang ZQ and Jia XH. 2008. Geochronological age and tectonic background of the Dabate A-type granite pluton in the west Tianshan. *Acta Petrologica Sinica*, 24(5):947–958

Abstract The Dabate granitic porphyry pluton is located geographically to the north of the Sayram Lake, western Tianshan and, tectonically, occurs in the orogenic belt between the Junggar plate to the north and the Yli-central Tianshan plate to the south. It mainly consists of biotite-bearing granite porphyries that are geochemically similar to A-type granites. They have high SiO_2 (75.6% ~ 77.6%), alkalis ($\text{Na}_2\text{O} + \text{K}_2\text{O} = 8.27\% \sim 8.70\%$), $\text{Fe}/(\text{Fe} + \text{Mg})$ (0.91 ~ 0.98) and $(\text{Ga}/\text{Al}) \times 10^4$ (3.19 ~ 3.40) values, but low Al_2O_3 (12.04% ~ 12.91%) and CaO (0.28% ~ 0.34%) contents. They are enriched in large ion lithophile elements (Rb, Th and U) and high field strength elements (Nb, Ta, Zr and Hf), but have obvious negative Eu, Ba and Sr anomalies and “sea-gull”-type rare earth element pattern. They also have relatively high Rb/Nb and Y/Nb ratios, indicating A_2 -type granite characteristics. Our new zircon LA-ICP-MS U-Pb age data suggest that the Dabate A-type granite porphyries were generated in the Early Permian ($288.9 \pm 2.3\text{Ma}$). Some residual zircon cores have a Late Carboniferous ($319.0 \pm 4.7\text{Ma}$) age, indicating that the source of the granitic porphyries likely contains Carboniferous magmatic rocks. Taking into account regional geological and magmatic rock data, we suggest that the northern Tianshan was in an extensional setting by the Early Permian, which was possibly related to post-collisional evolution of the orogenic belt.

Key words Zircon LA-ICPMS U-Pb dating; A-type granite; Post-collision; West Tianshan

摘要 达巴特花岗岩斑岩侵入体位于西天山北部的赛里木湖北部, 构造上属于准葛尔板块与伊犁-中天山板块之间的造山带。达巴特花岗岩斑岩具有 A 型花岗岩的特征, 如高硅 ($\text{SiO}_2 = 75.38\% \sim 77.61\%$)、碱 ($\text{Na}_2\text{O} + \text{K}_2\text{O} = 8.26\% \sim 10.10\%$) 和 $\text{Fe}/(\text{Fe} + \text{Mg})$ (0.91 ~ 0.98), 但低 Al_2O_3 (12.04 ~ 12.91%) 和 CaO (0.03% ~ 0.42%), 富集 Rb、Th、U 等大离子亲石元素和 Nb、Ta、Zr、Hf 等高场强元素, $(\text{Ga}/\text{Al}) \times 10^4$ 值变化于 3.19 ~ 3.40 之间, 具有明显的负 Eu、Ba 和 Sr 异常, 稀土配分显示“海鸥型”特征。达巴特花岗岩斑岩具有较高的 Rb/Nb 和 Y/Nb 比值, 显示了 A_2 型花岗岩的特征。LA-ICP-MS 锆石 U-Pb 测年结果显示达巴特岩体的侵位年龄为 $288.9 \pm 2.3\text{Ma}$, 并且一些锆石具有老的核 (319.0 ± 4.7), 暗示花岗岩斑的源岩中可能包含有石炭纪的岩浆岩。结合区域地质和岩浆岩资料, 我们认为西天山早二叠世处于伸展的背景中, 可能与造山带后碰撞阶段的演化有关。

* 国家重点基础研究发展规划项目(2007CB411308)、国家自然科学基金项目(40721063、40673037 和 40572042)和中国科学院知识创新项目(KZCX2-YW-128)的资助。

第一作者简介: 唐功建, 男, 1979 年生, 博士研究生, 岩石地球化学专业。

** 通讯作者: 王强, 男, 1971 年生, 博士, 研究员, E-mail: wqiang@gig.ac.cn

关键词 LA-ICPMS 锆石 U-Pb 定年; A 型花岗岩; 后碰撞; 西天山

中图法分类号 P588.121; P597.3

1 引言

近东西走向的天山造山带位于中亚造山带 (Coleman, 1989; Jahn *et al.*, 2000; Khain *et al.*, 2003) 或阿尔泰构造拼贴带 (Sengor *et al.*, 1993; Yakubchuk, 2004) 的最南端, 是哈萨克斯坦和塔里木板块的汇聚地带, 也是一个重要的 Cu-Au 等多金属成矿带。天山造山带是在古生代由塔里木和西伯利亚板块之间的古亚亚洲洋的消减闭合, 塔里木、准噶尔、哈萨克斯坦等板块的俯冲—碰撞—增生所形成 (Allen *et al.*, 1993; Coleman, 1989; Gao *et al.*, 1998; Sengor *et al.*, 1993; Shi *et al.*, 1994; Windley *et al.*, 1990; Xiao *et al.*, 2004a; Liu and Fei, 2006; Qian *et al.*, 2008)。但是, 目前对天山造山带的形成与演化, 尤其是晚古生代石炭纪—二叠纪的构造动力学背景还存有激烈的争论: 一是天山北部石炭纪是岛弧环境 (Zhu *et al.*, 2005; Zhang *et al.*, 2006a; Wang *et al.*, 2007b; 王强等, 2006)、碰撞后 (Wang *et al.*, 2004a; 韩宝福等, 2004; 王京彬和徐新, 2006)、还是裂谷环境 (Xia *et al.*, 2004b, 2008; 车自成和刘良, 1996; 顾连兴等, 2000) 或与地幔柱有关 (Pirajno *et al.*, 2008; 夏林圻等, 2004); 二是古生代北天山洋或准噶尔洋的闭合时限最终是在晚石炭—早二叠世关闭 (Allen *et al.*, 1993; Windley *et al.*, 1990; Xiao *et al.*, 2004b; Wang *et al.*, 2007b; 王强等, 2006) 或晚二叠 (Xiao *et al.*, 2008), 还是在石炭纪前 (Wang *et al.*, 2004a; Xia *et al.*, 2004b; 夏林圻等, 2002; 韩宝福等, 2004)。

达巴特矿区位于西天山赛里木湖北部。一些学者对其矿床成因、构造背景和成矿年代 (王志良等, 2004, 2006; 王核和彭省临, 2000; 张作衡等, 2006) 进行了研究, 认为: (1) 达巴特矿主要为铜铅矿床; (2) 矿化或矿区岩浆岩的时代为海西中期; (3) 矿床和区内岩浆岩的构造背景为阿拉套—科古琴晚古生代岛弧。达巴特矿区出露有许多岩浆岩, 通过对其深入研究, 有可能对深入了解金属矿床的成因和大地构造背景提供重要的启示。为此, 我们近期对达巴特矿区的花岗斑岩体进行了系统的主量、微量元素分析, 并对其进行了锆石 LA-ICP-MS U-Pb 同位素定年, 发现达巴特花岗斑岩体形成于早二叠世, 且显示了 A 型花岗岩的地球化学特征。本文将重点报道这一成果, 并来探讨其形成的构造背景。

2 地质背景与岩相学

中国境内天山造山带以乌鲁木齐为界 (东经 88° 线) 分为东天山和西天山。天山造山带分别以南天山和北天山两条晚古生代缝合线将其与塔里木和准噶尔两板块分开

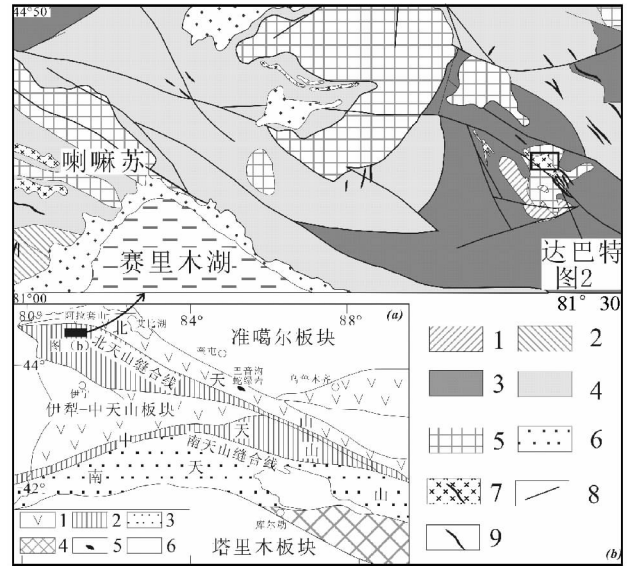


图 1 (a) 天山地区大地构造简图 (根据 Gao *et al.*, 1998 修改), 1-晚古生代火山岩或火山碎屑岩; 2-前寒武基底、古生代花岗岩和地层; 3-古生代沉积岩; 4-前寒武角闪岩相岩石; 5-蛇绿岩; 6-中生代地层; (b) 西天山达巴特地区地质简图 (根据新疆地质局第一区调队 1992 年温泉幅 1:20 万地质图改绘)。1-下元古界温泉群, 2-中元古界, 3-泥盆纪, 4-石炭纪, 5-二叠纪, 6-第四系, 7-花岗岩类, 8-断层; 9-花岗质脉岩

Fig. 1 (a) Simplified geological map of the western Tianshan (modified after Gao *et al.*, 1998); (b) Regional geological sketch map of the Lamasu and Dabate areas, western Tianshan (modified after 1:20000 geological map of Wenquan by the Xinjiang Geological Survey Team in 1992

(Windley *et al.*, 1990)。达巴特矿区所在的赛里木湖—博罗科努地区位于伊犁中天山板块的北缘, 北天山岛弧带和北天山缝合线的南侧 (图 1a)。研究区附近的温泉、赛里木湖地区出露以花岗片麻岩和斜长角闪岩为主的古—中元古 (2.1~1.7Ga) 基底, 古元古界的温泉群混合岩化片麻岩中锆石 U-Pb 年龄为 $798 \pm 8\text{Ma}$ 和 $821 \pm 11\text{Ma}$ (图 1b) (Hu *et al.*, 2000; 胡霁琴和等, 2001; 陈义兵等, 1999)。

达巴特矿区出露的地层主要为上泥盆统托斯库尔他乌组凝灰岩和凝灰质熔岩, 中部出露一长约 2km、宽 120m~500m 的酸性浅成侵入岩体, 岩性为流纹质凝灰角砾岩、流纹斑岩、花岗斑岩以及超浅成英安斑岩, 花岗斑岩和流纹质晶屑凝灰岩呈渐变过渡关系 (图 2)。前人报道了达巴特矿区花岗斑岩和英安斑岩中的锆石 SHRIMP U-Pb 年龄分别为 $317 \pm 8\text{Ma}$ 和 $315.9 \pm 5.9\text{Ma}$, 但没有原始数据 (王志良等,

2006)。矿体一般产于流纹质晶屑凝灰岩和角砾岩的接触带中,一般长 60m~300m,宽 1m~16m,呈细脉浸染状、脉状和透镜状产出(图 2)。辉钼矿 Re-Os 年龄为 $301 \pm 20\text{Ma}$ (张作衡等, 2006)。达巴特英安斑岩在区内东南边出露较多(图 2)。

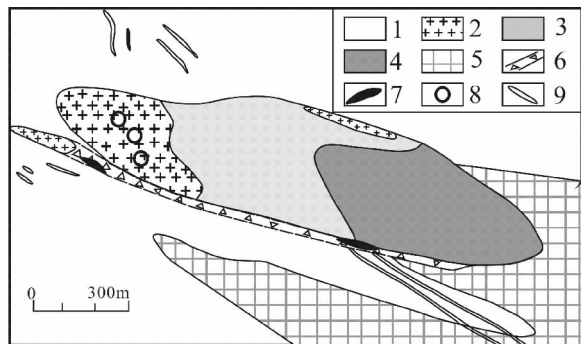


图 2 达巴特矿区地质简图(关明珍等^①修改)

1-上泥盆系托斯库尔他乌组; 2-花岗岩斑岩; 3-流纹质质屑凝灰岩; 4-流纹质质熔结凝灰岩; 5-英安斑岩; 6-破碎带; 7-铜钼矿体; 8-采样点; 9-石英斑岩脉

Fig. 2 Geological sketch map of the Dabate copper deposit (after Guan *et al.*)

本文研究的重点是与矿化关系并不密切的花岗斑岩侵入体(图 2)。该侵入体侵入上泥盆系托斯库尔他乌组。花岗岩斑岩为土红色、砖红色,斑状结构,块状构造,斑晶占 10%~15%,自形、半自形板状,成分为斜长石、石英、钾长石和少量黑云母,粒径 1mm~3mm,基质 85%~90%,主要成分为石英、钾长石、斜长石、次为少量黑云母,构成显微花岗岩结构。

3 分析方法

主、微量元素的分析测试均在中国科学院广州地球化学研究所同位素年代学和地球化学重点实验室完成。主量元素分析是用 Rigaku RIX 2000 型荧光光谱仪(XRF)分析,其详细步骤与 Li *et al.* (2005)所述相同。样品的含量由 36 种涵盖硅酸盐样品范围的参考标准物质双变量拟合的工作曲线确定,基体校正根据经验的 Traill-Lachance 程序进行,分析精度优于 1%~5%。微量元素的分析则采用 Perkin-Elmer Sciex ELAN 6000 型电感耦合等离子体质谱仪(ICP-MS),具体的流程见 Li(1997)。使用 USGS 标准 W-2 和 G-2 及国内标准 GSR-1、GSR-2 和 GSR-3 来校正所测样品的元素含量,分析精度一般为 2%~5%。分析数据列于表 1。

为精选锆石样品,先将新鲜的岩石样品粉碎至 120 目以下,用常规的人工淘洗和电磁选方法富集锆石,再在双目镜下用手工方法逐个精选锆石颗粒,未用任何化学试剂。本次锆石定年样品和主元素和微量元素分析的样品相对应。

表 1 达巴特花岗斑岩主量(wt%)、微量元素($\times 10^{-6}$)组成
Table 1 Major element (wt%) and trace element ($\times 10^{-6}$) compositions of the Dabate granitic porphyries

	06-XJ-08	06XJ-10	06XJ-12	06XJ-13	06-XJ-14	06XJ-15
SiO ₂	75.56	75.67	76.92	76.36	75.38	77.61
TiO ₂	0.08	0.12	0.09	0.11	0.10	0.10
Al ₂ O ₃	12.80	12.04	12.91	12.72	12.64	12.97
Fe ₂ O ₃	1.16	1.14	0.95	1.28	1.17	0.97
MnO	0.002	0.002	0.003	0.004	0.004	0.003
MgO	0.05	0.05	0.01	0.01	0.06	0.01
CaO	0.03	0.03	0.28	0.34	0.42	0.31
Na ₂ O	2.47	1.39	3.00	3.56	4.06	3.27
K ₂ O	7.63	8.08	5.27	5.14	4.92	5.21
P ₂ O ₅	0.01	0.01	0.01	0.01	0.01	0.00
LOI	0.62	0.88	0.79	0.87	0.79	0.00
Total	100.40	99.41	100.21	100.40	99.54	100.14
Sc	0.121	0.0450	2.19	0.0420	0.849	0.137
V	9.09	15.6	3.95	7.98	19.6	7.36
Cr	4.20	8.43	15.6	2.51	7.25	12.2
Co	0.424	0.768	0.518	0.625	0.452	0.652
Ni	1.41	2.63	3.06	2.09	1.83	7.61
Ga	20.8	19.8	21.8	22.8	25.2	23.2
Cs	20.0	18.4	15.3	14.5	17.2	18.6
Rb	316	357	265	264	286	287
Ba	110	209	144	150	107	109
Th	15.4	13.0	20.2	15.3	18.7	12.5
U	3.72	2.92	3.38	2.38	2.50	7.44
Nb	25.2	20.6	24.8	25.6	27.5	24.2
Ta	2.29	1.82	2.18	2.04	2.28	2.10
Sr	35.1	29.3	22.8	27.1	18.6	17.9
Y	40.8	29.6	57.3	52.7	58.7	51.5
Zr	91.6	101	140	128	142	121
Hf	4.08	4.05	5.81	5.29	5.83	5.29
La	8.17	6.63	19.1	15.9	18.8	13.3
Ce	22.5	17.3	46.7	37.4	43.9	31.7
Pb	9.52	6.15	10.1	9.80	14.4	12.5
Pr	3.23	2.40	6.20	4.90	6.04	4.22
Nd	13.6	10.5	23.6	18.5	23.1	15.9
Sm	4.86	3.35	6.65	5.12	6.42	4.64
Eu	0.145	0.154	0.268	0.211	0.225	0.199
Gd	5.26	3.48	7.84	6.08	7.37	5.97
Tb	1.11	0.710	1.61	1.38	1.59	1.39
Dy	6.76	4.44	10.1	8.70	9.62	8.74
Ho	1.39	0.923	2.11	1.78	2.07	1.86
Er	3.74	2.64	5.94	5.06	5.76	5.28
Tm	0.575	0.428	0.919	0.729	0.873	0.787
Yb	3.67	2.73	5.80	4.78	5.47	4.87
Lu	0.517	0.409	0.887	0.687	0.788	0.720

① 关明珍等. 新疆赛里木湖铜多金属成矿带地物化探综合研究及靶区优选. 新疆 305 项目 N7-1 课题

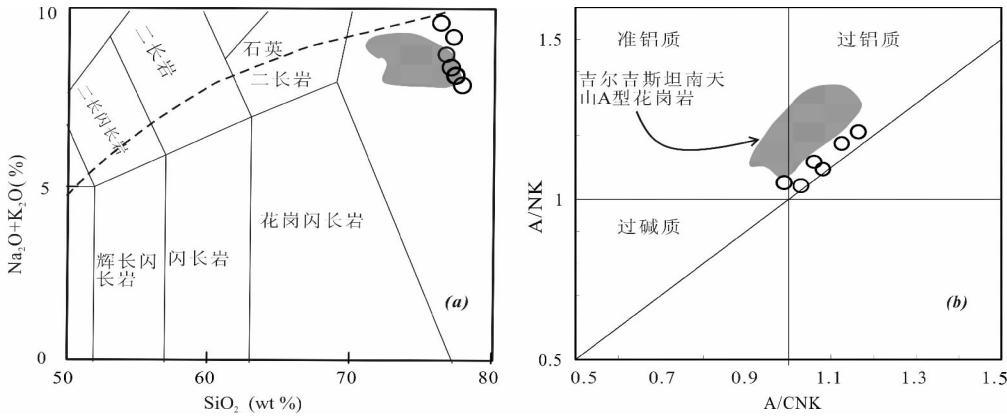


图3 TAS (a) (Middlemost, 1994) 和 A/CNK-A/NK 图解 (b), ($A/CNK = \text{molar} [Al_2O_3 / (CaO + Na_2O + K_2O)]$); $A/NK = \text{molar} Al_2O_3 / (Na_2O + K_2O)$) 吉尔吉斯斯坦南天山 A 型花岗岩来源于 (Konopelko *et al.*, 2007)

Fig. 3 TAS (a) and A/CNK-A/NK (b) digrams for the Dabate granite porphyries

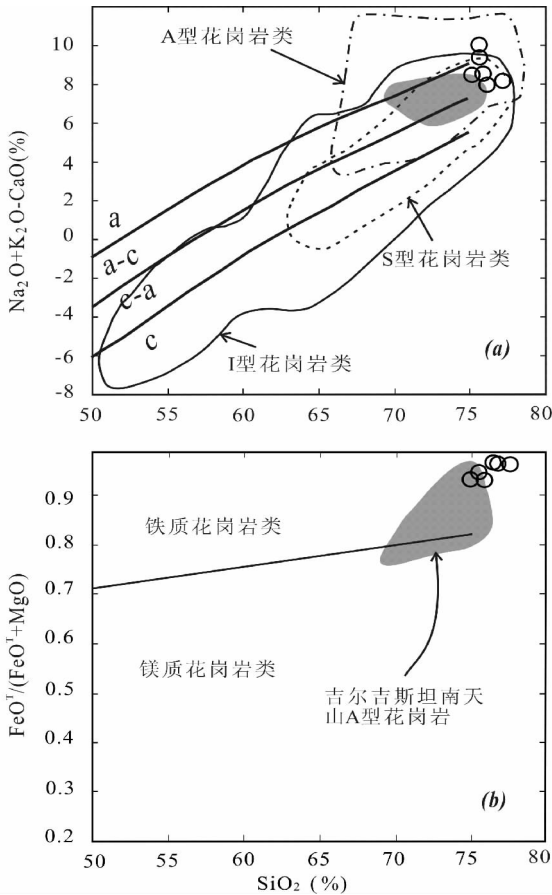


图4 (a) $(Na_2O + K_2O) - (CaO) - SiO_2\%$ 和 (b) $(FeO^T)/(FeO^T + MgO) - SiO_2\%$ 图 (据 Frost *et al.*, 2001) 吉尔吉斯斯坦南天山 A 型花岗岩来源于 (Konopelko *et al.*, 2007), c-钙性花岗岩类; c-a-钙碱性花岗岩类; a-c-碱钙性花岗岩类; a-碱性花岗岩类

Fig. 4 (a) $(Na_2O + K_2O) - (CaO) - SiO_2\%$ and (b) $(FeO^T)/(FeO^T + MgO) - SiO_2\%$ (after Frost *et al.*, 2001)

锆石阴极发光图像研究在中国科学院广州地球化学研究所 JXA-8100 电子探针仪上完成。锆石 LA-ICP-MS U-Pb 年龄测定在中国地质大学 (武汉) 地质过程与矿产资源国家重点实验室完成。ICP-MS 为 Perkin Elmer/SCIEX 公司带有动态反应池的四极杆 ICP-MS Elan6100DRC, 仪器依标准模式运行, 激光剥蚀系统为德国 Lamda Physik 公司的 GeoLas 200M 深紫外 (DUV) 193nm ArF 准分子 (excimer) 激光剥蚀系统。实验中采用 He 作为剥蚀物质的载气, 激光斑束直径为 32 μm 。参考物质为美国国家标准技术协会研制的人工合成硅酸盐玻璃 NIST SRM610, 锆石 U-Pb 年龄的测定采用国际标准锆石 91500 作为外标校正方法, 每隔 5 个分析点测一次标准, 保证标准和样品的仪器条件完全一致。在样品分析前后以及每隔 20 个测点各测一次 NIST SRM610, 以 Si 做内标, 测定锆石中的 U, Th, Pb 的含量。详细的分析流程及有关参数见 (Yuan *et al.*, 2004)。元素的比率和元素的含量用 GLITTER (4.0 版) 来处理, 年龄的计算和谐和图用 ISOPLOT (3.00 版) (Ludwig, 2003) 来完成。分析数据列于表 2。

4 花岗斑岩的元素地球化学特征

达巴特花岗斑岩高硅, SiO_2 含量变化范围小 (75.38% ~ 77.61%), Al_2O_3 含量为 12.04% ~ 12.91%, $K_2O + Na_2O$ 含量为 8.26% ~ 10.10%, K_2O/Na_2O 为 1.2 ~ 5.8。在 TAS 图解 (图 3a) 中岩石样品落入花岗岩区, 并落入亚碱性区, 弱过铝质, 铝饱和度 A/CNK 为 0.99 ~ 1.12 (图 3b)。花岗斑岩具有高的 $Fe/(Fe + Mg)$, 约 0.98, 根据 Frost *et al.* (2001) 的花岗岩分类, 岩石样品落在铁质范围和钙碱性内 (图 4)。达巴特花岗斑岩富集高场强元素 (Zr, Hf, Nb, Ta、重稀土元素和大离子亲石头 (U, Th), 稀土元素轻重稀土无分馏, 配分模式呈海鸥状 (图 5a), $(La/Yb)_N$ 为 2.3 ~ 2.5, 具有明显的负 Eu、Ba、Sr 异常和 Nb 正异常 (图 5b)。

表 2 达巴特花岗岩锆石 LA-ICPMS 分析结果
Table 2 Zircon LA-ICPMS analyzing results for the granitic porphyries in the Dabate areas

分析点号	元素含量($\times 10^{-6}$)		元素比值		同位素比值				表观年龄(Ma)						
	Th^{232}	U^{238}	U/Th	$^{207}Pb/^{206}Pb$	1 σ	$^{207}Pb/^{235}U$	1 σ	$^{206}Pb/^{238}U$	1 σ	$^{207}Pb/^{206}Pb$	1 σ	$^{207}Pb/^{235}U$	1 σ	$^{206}Pb/^{238}U$	1 σ
06XJ013-1	61	105	1.72	0.05397	0.00238	0.37540	0.01586	0.05045	0.00064	370	102	324	12	317	4
06XJ013-2	193	358	1.86	0.07118	0.00116	0.45377	0.00749	0.04623	0.00052	963	17	380	5	291	3
06XJ013-3	146	290	1.99	0.05402	0.00166	0.34298	0.00980	0.04604	0.00053	372	71	299	7	290	3
06XJ013-4	302	509	1.69	0.05359	0.00072	0.34155	0.00473	0.04622	0.00051	354	14	298	4	291	3
06XJ013-5	29	61	2.08	0.05311	0.00138	0.33785	0.00873	0.04614	0.00056	333	37	296	7	291	3
06XJ013-6	79	155	1.96	0.05310	0.00196	0.37170	0.01301	0.05077	0.00061	333	86	321	10	319	4
06XJ013-7	50	175	3.51	0.05339	0.00099	0.33923	0.00633	0.04609	0.00052	345	23	297	5	290	3
06XJ013-8	356	677	1.90	0.05327	0.00077	0.33625	0.00501	0.04578	0.00050	340	16	294	4	289	3
06XJ013-9	324	545	1.68	0.05314	0.00070	0.34021	0.00466	0.04643	0.00051	335	14	297	4	293	3
06XJ013-10	455	615	1.35	0.06762	0.00272	0.41114	0.01572	0.04410	0.00055	857	86	350	11	278	3
06XJ013-11	106	190	1.79	0.05341	0.00107	0.37410	0.00751	0.05079	0.00058	346	25	323	6	319	4
06XJ013-12	137	221	1.61	0.05675	0.00093	0.36120	0.00599	0.04616	0.00051	482	19	313	4	291	3
06XJ013-13	256	317	1.24	0.05244	0.00077	0.33593	0.00504	0.04646	0.00051	305	16	294	4	293	3
06XJ013-14	850	1616	1.90	0.06358	0.00600	0.33191	0.03097	0.03786	0.00054	728	208	291	24	240	3
06XJ013-15	65	169	2.61	0.05196	0.00094	0.33400	0.00612	0.04662	0.00053	284	22	293	5	294	3
06XJ013-16	89	167	1.88	0.05841	0.00238	0.35907	0.01394	0.04458	0.00056	545	91	312	10	281	3
06XJ013-17	645	1253	1.94	0.06261	0.00092	0.36572	0.00551	0.04236	0.00047	695	15	316	4	267	3
06XJ013-18	139	499	3.59	0.05614	0.00079	0.39290	0.00569	0.05075	0.00056	458	15	336	4	319	3
06XJ013-19	669	663	0.99	0.06496	0.00090	0.40648	0.00580	0.04538	0.00050	773	14	346	4	286	3
06XJ013-20	290	460	1.59	0.05735	0.00200	0.35351	0.01162	0.04470	0.00052	505	79	307	9	282	3
06XJ013-22	199	414	2.08	0.06178	0.00091	0.39809	0.00600	0.04673	0.00052	667	15	340	4	294	3
06XJ013-23	349	644	1.84	0.05353	0.00078	0.34120	0.00509	0.04622	0.00051	351	16	298	4	291	3
06XJ013-24	178	365	2.05	0.05154	0.00161	0.32488	0.00942	0.04572	0.00053	265	73	286	7	288	3
06XJ013-25	139	383	2.76	0.05433	0.00080	0.34127	0.00515	0.04556	0.00050	385	16	298	4	287	3

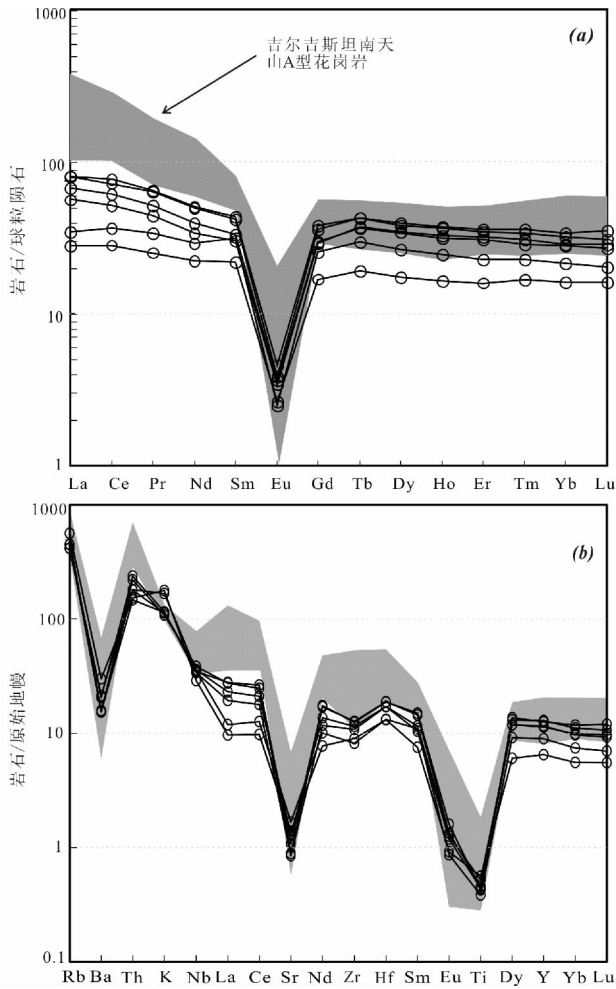


图5 稀土元素球粒陨石标准化配图(a)和微量元素NMORB标准化蛛网图(b)(标准值据(Sun and McDonough, 1989))

吉尔吉斯斯坦南天山A型花岗岩来源于(Konopelko *et al.*, 2007)

Fig. 5 The chondrite-normalized rare earth element (REE) patterns (a) and primitive mantle-normalized multi-element plots (b) (normalized values from (Sun and McDonough, 1989))

5 锆石 LA-ICPMS U-Pb 定年

达巴特花岗岩斑岩样品 06XJ-013 的绝大多数的锆石呈棱柱状,长约 $40\mu\text{m} \sim 130\mu\text{m}$,长宽比在 $1:1.5 \sim 3:1$,少量呈浑圆状。阴极发光图像(图6)显示发育有清晰的韵律结构,为典型的岩浆锆石。锆石的 U、Th 含量较高,分别可达 1616×10^{-6} 和 850×10^{-6} 。锆石具有比较均一的 U/Th 比 ($0.9 \sim 2.7$),大部分在 $1 \sim 2$ 之间,为典型的岩浆锆石。24 个分析点中有 18 个在 $278 \sim 294\text{Ma}$ 之间(图6),其加权平均值为 $288.9 \pm 2.3\text{Ma}$,其中有几个点偏离谐和线,这可能是由于不同程度的普通 Pb 的贡献,或者是结晶后 U 和 Pb 同位素的

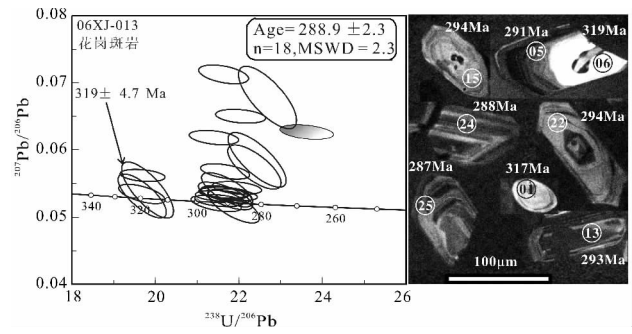


图6 06XJ-013 U-Pb 年龄谱和锆石阴极发光图像

Fig. 6 Concordia diagram showing LA-ICPMS analytical points for zircons from the Dabate granite porphyries and CL images

增加或丢失,这种不一致往往是由于测量时 ^{207}Pb 偏高,但当锆石年龄小于 1000Ma 时一般不影响 $^{206}\text{Pb}/^{238}\text{U}$ 年龄。另有 4 个分析点落在 320Ma 的谐和线附近,其加权平均值为 $319.0 \pm 4.7\text{Ma}$,这组锆石的形态和其它锆石明显不同,或出现于锆石核部(边部时代为 $\sim 290\text{Ma}$)或呈现出浑圆状,我们把它解释为石炭纪火山岩的捕获晶或花岗斑岩的源岩锆石熔蚀后的残留体(后面详细讨论)。还有两个分析点(14、17)明显偏离谐和线并小于 280Ma ,可能反映了锆石在形成过程中有 Pb 丢失。

6 讨论

6.1 形成时代

前人曾对达巴特花岗岩斑岩和英安斑岩进行了 SHRIMP 锆石 U-Pb 定年,结果分别为 $317 \pm 8\text{Ma}$ 和 $315.9 \pm 5.9\text{Ma}$ (无原始数据)(王志良等, 2006; 张作衡等, 2006),这和我们本次定年结果中年龄较老的年龄为 $319.0 \pm 4.7\text{Ma}$ 一组数据相一致。结合锆石 CL 图像(图6)可以看出, 319Ma 这一组数据的锆石或者为锆石的核部,或者是那些韵律结构模糊并呈现出浑圆状的锆石,如同一颗锆石中核部年龄为 319Ma ,边部年龄为 291Ma 。因此,我们认为晚石炭世($317 \sim 319\text{Ma}$)年龄很可能是来自晚石炭世火成岩锆石捕获晶或花岗斑岩源岩锆石熔蚀后的残留体,并且后一种可能性更大。早二叠世($\sim 289\text{Ma}$)的锆石均为棱柱状,晶型较好,CL 图像中显示有清晰的韵律环带, U/Th 为 $0.9 \sim 2.7$,为典型的岩浆锆石,所以该组年龄代表了岩体的结晶年龄。该地区广泛发育晚石炭世—二叠世岩浆岩:博罗科努山闪长岩 SHRIMP 锆石 U-Pb 年龄为 $308.2 \pm 5.4\text{Ma}$ (朱志新等, 2006),辉石闪长岩 LA-ICP-MS 锆石 U-Pb 年龄为 $301 \pm 7\text{Ma}$,黑云母花岗岩年龄范围为 $294 \pm 7 \sim 285 \pm 7\text{Ma}$,黑云母钾长花岗岩形成于 $280 \pm 5 \sim 266 \pm 6\text{Ma}$ (王博等, 2007),玉希莫洛盖达坂花岗闪长岩 LA-ICP-MS 锆石 U-Pb 年龄为 $315 \pm 3\text{Ma}$ 和 $309 \pm 3\text{Ma}$ (Wang *et al.*, 2006a),哈希勒根达坂黑云母花岗岩 TIMS 锆石 U-Pb

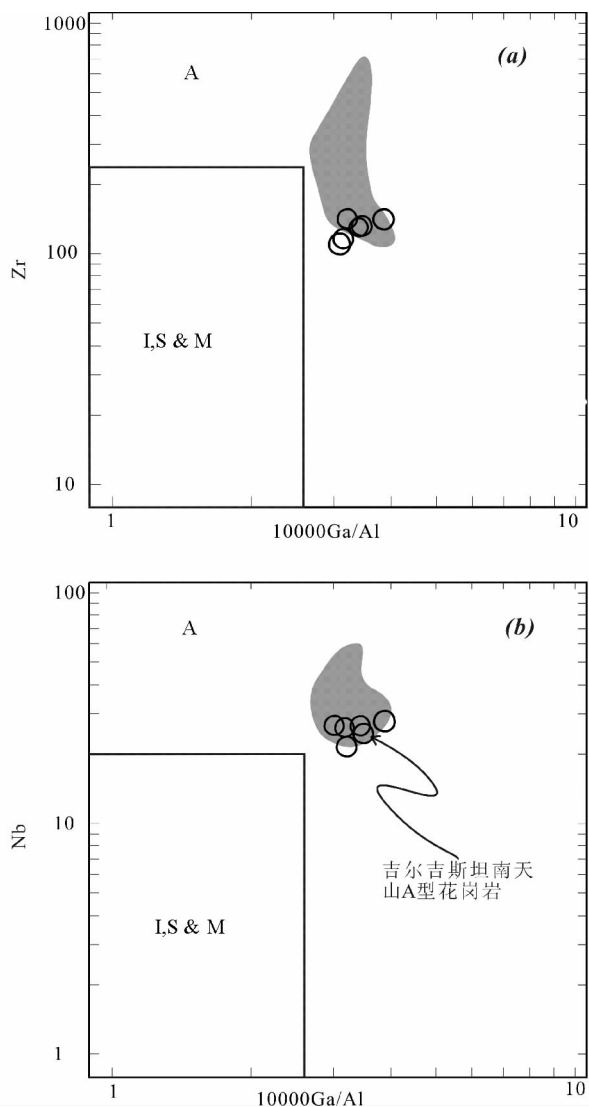


图7 达巴特花岗斑岩 $10000 \times \text{Ga}/\text{Al}$ 对 Zr(a) 和 Nb(b) 图解(据(Whalen *et al.*, 1987))

吉尔吉斯斯坦南天山 A 型花岗岩来源于(Konopelko *et al.*, 2007), I, S & M-未分异的 I, S 和 M 型花岗岩, A-A 型花岗岩

Fig. 7 $10000 \times \text{Ga}/\text{Al}$ versus Zr (a) and Nb (b) digrams for the Dabate granite porphyries (after Whalen *et al.*, 1987)

年龄为 $286.8 \pm 0.8\text{Ma}$ (徐学义等, 2006c)。因此,西天山伊犁板块北缘的岩浆岩主要形成于晚古生代,而达巴特岩体形成于古生代晚期的早二叠世。

6.2 岩石类型与成因

达巴特花岗斑岩具有 A 型花岗岩的特点:(1)富硅、富碱,贫镁,具有高的 $\text{Fe}/(\text{Fe} + \text{Mg})$; (2)富集 Rb、Th、U 等大离子亲石元素和 Nb、Ta、Zr、Hf 等高场强元素,亏损 Sr、Ba(图 5b),富 Ga(图 7), $(\text{Ga}/\text{Al}) \times 10^4$ 值变化于 $3.19 \sim 3.40$

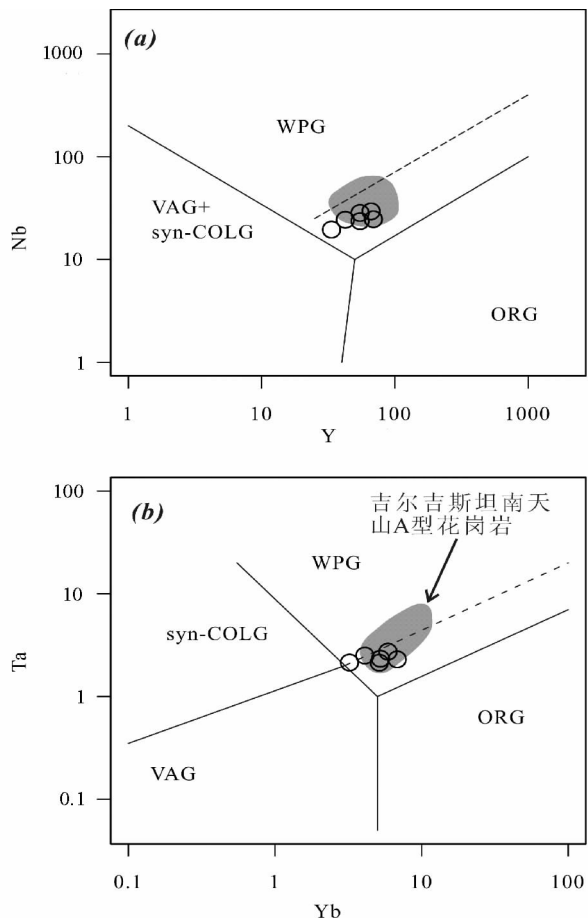


图8 达巴特斑岩 Y-Nb (a) 和 Yb-Ta (b) 构造环境判别图解(据 Pearce *et al.*, 1984)

吉尔吉斯斯坦南天山 A 型花岗岩来源于(Konopelko *et al.*, 2007), syn-COLG-同碰撞型; VAG-火山弧型; WPG-板块内部型; ORG-洋中脊型

Fig. 8 Y-Nb (a) and Yb-Ta (b) tectonic discrimination digrams for the Dabate granite porphyry (after Pearce *et al.*, 1984)

之间。在 Whalen *et al.* (1987) 以 $10000 \times \text{Ga}/\text{Al}$ 比值为标准的花岗岩分类图上,花岗斑岩投影在 A 型花岗岩区(图 7),与铝质 A 型花岗岩相一致(图 3b)(King *et al.*, 1997),和吉尔吉斯斯坦南天山早二叠世(280 ~ 296Ma) A-型花岗岩(Konopelko *et al.*, 2007)相似(图 3,4,6,7,8,9)。高硅的铝质 A 型花岗岩经常与高分异的 I 型花岗岩表现出相似的特点(King *et al.*, 1997),二者很难区分(吴福元等,2007)。但达巴特花岗斑岩很可能是 A 型花岗岩而不是高分异的 I 型花岗岩:如高分异的 I 型花岗岩的形成温度为 764°C (King *et al.*, 1997),而达巴特花岗斑岩的锆石饱和温度为 $783 \sim 822^\circ\text{C}$;高分异的 I 型花岗岩的 FeO 的含量含量往往较低($\sim 0.5\%$),而达巴特 A 型花岗岩的 FeO 的含量较高($0.85 \sim 1.04\%$)。在 Y-Nb 和 Yb-Ta 判别图(图 8)中,同典型 A 型花岗岩一样,达巴特花岗斑岩落入板内花岗岩区。Eby

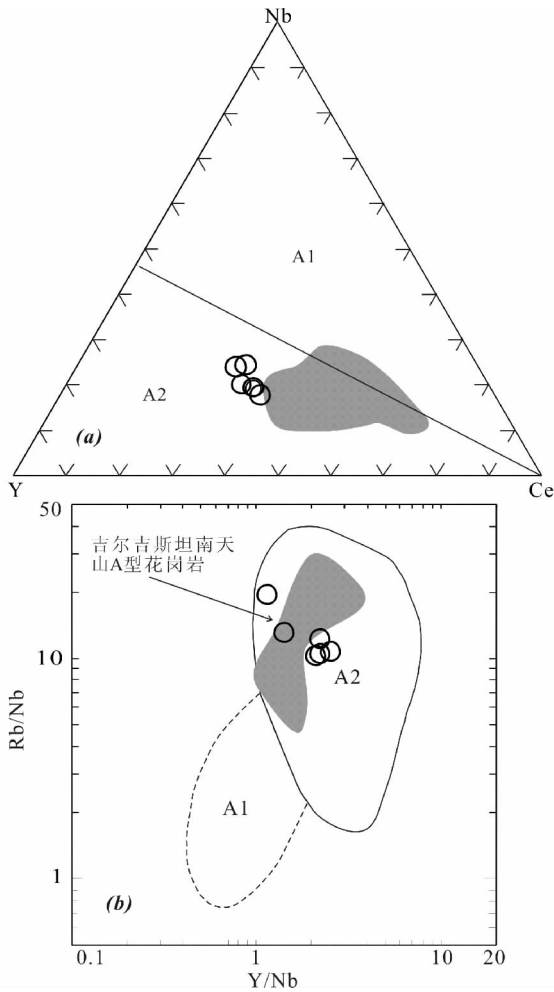


图9 达巴特花岗斑岩 Y-Nb-Ce (a) 和 Rb/Nb-Y/Nb (b) 图解 (据 Eby, 1992)

吉尔吉斯斯坦南天山 A 型花岗岩来源于 (Konopelko *et al.*, 2007)

Fig. 9 Y-Nb-Ce (a) and Rb/Nb-Y/Nb (b) digrams for the Dabate granite porphyries (after Eby, 1992)

(1992) 根据地球化学特征将 A 型花岗岩分为 A₁ 和 A₂ 型, 并认为 A₁ 型是地幔来源, 且侵位于大陆裂谷或板内的构造环境, A₂ 型来源于大陆地壳或板内下地壳, 主要形成于后碰撞环境。达巴特花岗斑岩在 Y-Nb-Ce 和 Y/Nb-Rb/Nb 判别图中均投影于 A₂ 区 (图 9)。

前人对于 A 型花岗岩的成因提出了许多模式: (1) 地幔玄武质岩浆高度结晶分异 (Beyth *et al.*, 1994; Han *et al.*, 1997; Mushkin *et al.*, 2003; Turner *et al.*, 1992); (2) 各种源岩的部分熔融, 如麻粒岩相岩石 (Clemens *et al.*, 1986; Collins *et al.*, 1982; King *et al.*, 1997; Whalen *et al.*, 1987)、英云闪长岩-花岗闪长岩 (Creaser *et al.*, 1991) 和紫苏花岗岩 (Landenberger and Collins, 1996)、新生玄武质地壳 (Wu *et al.*, 2002); (3) 幔源物质和壳源物质混合 (Konopelko *et al.*, 2007; Mingram *et al.*, 2000; Yang *et al.*, 2006a; 邱检生等, 1999); (4) 上地壳钙碱性岩石低压熔融

(Patino Douce, 1997)。由于还缺乏详细的 Sr-Nd 同位素资料, 我们还不能对达巴特花岗斑岩的源岩或成因模式进行准确的限制。但是达巴特花岗斑岩并不与同期玄武质岩石密切共生, 因此我们认为其由地幔玄武质岩浆高度结晶分异形成的可能性较小。此外, 达巴特花岗斑岩中存在的晚石炭世 (319.0 ± 4.7 Ma) 的熔蚀残留锆石核, 暗示其源区很可能与晚石炭世事件有关。由于石炭纪可能是天山北部地区重要的岛弧岩浆活动时期 (Wang *et al.*, 2007b; 王强等, 2006), 如博罗科努、玉希莫洛盖达坂等岩体均为石炭纪岩浆 (Wang *et al.*, 2006a; 朱志新等, 2006)。因此斑岩中存在的晚石炭世 (319.0 ± 4.7 Ma) 的年龄可能暗示达巴特斑岩的源岩中包含石炭纪的岛弧岩浆岩。在早二叠世, 西天山北部很可能已经进入碰撞后伸展阶段, 达巴特花岗斑岩可能是在早二叠世后碰撞岩石圈伸展的背景下形成: 岩石圈伸展促使软流圈上涌并加热中下地壳物质, 导致石炭纪底侵的岛弧岩浆岩发生熔融形成 A 型花岗岩。这与典型 A₂ 型花岗岩的形成模式 (Eby, 1992) 比较一致。

6.3 动力学意义

中国境内天山造山带以乌鲁木齐为界 (东经 88° 线) 分为东天山和西天山。天山造山带分别以南天山和北天山两条晚古生代缝合线将其与塔里木和准噶尔两板块分开 (图 1a) (Windley *et al.*, 1990)。南天山缝合线为位于塔里木板块和伊犁中天山板块之间的古南天山洋俯冲于伊犁中天山板块的缝合线, 一般认为其在早石炭世闭合 (Allen *et al.*, 1993; Carroll *et al.*, 1995; Coleman, 1989; Gao *et al.*, 1998; 高俊等, 2006), 但也有学者认为闭合在石炭世之前 (Xia *et al.*, 2004b) 或三叠纪 (Zhang *et al.*, 2007a, 2007b), 北天山缝合线为准噶尔洋 (又称北天山洋) 向南俯冲于伊犁中天山板块的缝合线, 一般认为闭合于早石炭世或晚石炭世 (Allen *et al.*, 1993; Carroll *et al.*, 1995; Coleman, 1989; Gao *et al.*, 1998; Wang *et al.*, 2007b)。北天山和南天山主要由活动增生带、大陆边缘和岛弧组成等组成 (Gao *et al.*, 1995, 1998), 中天山主要有各种变质岩和深海和浅海沉积物 (Xiao *et al.*, 2008)。

天山造山带是在晚古生代由准噶尔、伊犁中天山和塔里木板块碰撞作用而形成 (Gao *et al.*, 1998)。许多学者认为准噶尔洋从奥陶世 (龙灵利, 2007)、晚泥盆世 (Wang *et al.*, 2006a)、或晚石炭世早期 (Wang *et al.*, 2007b) 向南俯冲于伊犁中天山板块之下, 于晚石炭世闭合 (Allen *et al.*, 1993; Carroll *et al.*, 1995; Coleman, 1989; Wang *et al.*, 2007b)。其中西天山北部的岩浆岩主要形成于古生代, 在 370 ~ 260 Ma 之间 (图 10), 其中分别主要集中在 370 ~ 350 Ma 和 320 ~ 280 Ma 两个时间段, 其中后者又分为 320 ~ 300 Ma 和 300 ~ 280 Ma 两个阶段, 所以西天山北部泥盆纪-二叠纪岩浆岩可以分为三期, 即晚泥盆世-早石炭世、晚石炭世和早二叠世。其中晚泥盆世-早石炭世形成的如莱历斯高尔岩

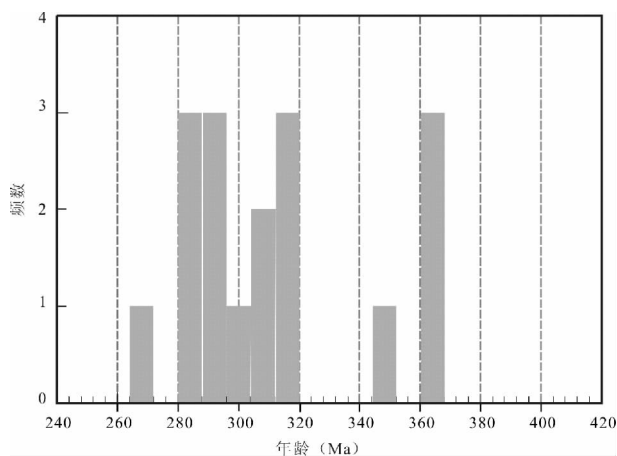


图 10 西天山伊犁中天山板块北缘岩浆岩年龄统计图

数据来源于(Wang *et al.*, 2006a; Zhao *et al.*, 2008; 王志良等, 2006; 王博等, 2007; 朱志新等, 2006; 李华芹等, 2006; 唐功建等, 2008; 徐学义等, 2006c; 翟伟等, 2006)

Fig. 10 Age histograms for the igneous rocks in the northern margin of the Yili-central Tianshan Plate

体(李华芹等, 2006); 晚石炭世之间形成的如博罗科努山岩体(Wang *et al.*, 2006a; 朱志新等, 2006); 早二叠世形成的岩体如达巴特岩体, 哈希勒根达坂岩体(徐学义等, 2006c)。前两期花岗岩类都具有岛弧或活动大陆边缘型花岗岩类的特点, 可能与准噶尔洋的俯冲消减有关, 形成于大陆弧或岛弧环境。我们最近发现达巴特以西的 40km 的喇嘛苏斑岩形成于晚泥盆世($366.3 \pm 1.9\text{Ma}$), 且与俯冲洋壳熔融形成的埃达克岩非常类似(唐功建等, 2008), 也进一步证实了该区晚泥盆世为岛弧环境。此外, 西天山北部的巴音沟蛇绿岩中堆晶辉长岩 LA-ICP-MS 锆石 U-Pb 年龄为 $344.0 \pm 3.4\text{Ma}$ (徐学义等, 2006a), 侵位于辉长岩中的斜长花岗岩 SHRIMP 锆石 U-Pb 年龄为 $324.7 \pm 7.1\text{Ma}$ (徐学义等, 2006b), 表明该蛇绿岩形成于早石炭世。最近的研究表明, 在天山北部地区也存在石炭纪的洋壳俯冲和熔融作用, 并且形成了典型的岛弧岩浆岩组合埃达克岩—高镁安山岩—富 Nb 玄武岩组合(Wang *et al.*, 2007b; 王强等, 2006)。所以晚石炭世的岩浆岩可能是由石炭纪北天山洋(准噶尔洋)向南俯冲到伊犁中天山板块作用形成的。早二叠世岩浆岩可能是在石炭纪北天山洋(准噶尔洋)闭合碰撞后的伸展背景下形成的。由于 A 型花岗岩多形成于拉张伸展的构造环境, 并经常出现在非造山或碰撞后伸展阶段(Black *et al.*, 1993; Clemens *et al.*, 1986; Eby, 1990, 1992; Whalen *et al.*, 1987; Wu *et al.*, 2002), 所以达巴特 A 型花岗岩的出现标志着西天山伊犁中天山板块北缘的造山带可能已经进入在早二叠世进入伸展阶段, 很可能与造山带后碰撞的演化有关。本文报道的达巴特 A 型花岗岩的早二叠世的侵位年龄($288.9 \pm 2.3\text{Ma}$) 晚于准噶尔洋晚石炭世闭合的时限, 除了达巴特 A 型花岗岩外, 还有许多证据说明早二叠世伊犁中天山板块北缘的造山带

已经进入伸展阶段, 并可能与造山带后碰撞的演化有关: (1) 被认为是后碰撞造山环境下哈希勒根达坂的黑云母花岗岩形成时代为 $286.8\text{Ma} \pm 0.8$ (徐学义等, 2006c), 吉尔吉斯斯坦南天山的 A 型花岗岩的形成时代也形成于早二叠世($280 \sim 296\text{Ma}$)(Konopelko *et al.*, 2007); (2) 在天山地区二叠世也出现了双峰式火山岩(车自成等, 1994) 以及陆相磨拉石堆积(龙灵利, 2007) 等; (3) 塔里木西部的小海子正长岩(A 型花岗岩)的 SHRIMP 锆石 U-Pb 年龄为 $277 \pm 4\text{Ma}$ (Yang *et al.*, 2007; 杨树锋等, 2006)。

7 结论

(1) 达巴特岩体侵位于 $288.9 \pm 2.3\text{Ma}$, 为早二叠世岩体。

(2) 达巴特花岗岩斑岩具有 A (A_2) 型花岗岩的特点, 可能是石炭纪底侵于中下地壳中的岩浆岩在伸展的条件下熔融形成。

(3) 西天山伊犁中天山板块北缘的造山带在早二叠世为伸展环境, 可能与造山带后碰撞的伸展有关。

致谢 肖文交研究员、郭敬辉研究员和另一位匿名的审稿专家对本文提出了宝贵的建议。室内主量、微量元素分析得到了刘颖、胡光黔老师的帮助, 锆石年代学分析得到了刘勇胜教授和宗克清的帮助, 在此一并表示感谢!

References

- Allen MB, Windley BF and Zhang C. 1993. Palaeozoic collisional tectonics and magmatism of the Chinese Tien Shan, central Asia. *Tectonophysics*, 220(1-4): 89-115
- Beyth M, Stern RJ, Altherr R and Kroner A. 1994. The Late Precambrian Timna igneous complex, Southern Israel: Evidence for comagmatic-type sanukitoid monzodiorite and alkali granite magma. *Lithos*, 31(3-4): 103-124
- Black R and Liegeois JP. 1993. Cratons, mobile belts, alkaline rocks and continental lithospheric mantle: The Pan-African testimony. *Journal of the Geological Society* 150(1): 89-98
- Carroll AR, Graham SA, Hendrix MS, Ying D and Zhou D. 1995. Late Paleozoic tectonic amalgamation of northwestern China: Sedimentary record of the northern Tarim, northwestern Turpan, and southern Junggar basins. *Geol. Soc. Am. Bull.*, 107(5): 571-594
- Che ZL and Liu L. 1996. Review on the Ancient Yili Rift, Xingjian, China. *Acta Petrologica Sinica*, 12(3): 478-490 (in Chinese with English abstract)
- Che ZL, Liu HF and Liu L. 1994. Forming and evolution of the Middle Tianshan. Beijing: The Geological Publishing House Beijing, 135 (in Chinese)
- Chen YB, Hu A, Zhang GX and Zhang QF. 1999. Zircon U-Pb age and Nd-Sr isotopic composition of granitic gneiss and its geological implication from Precambrian window of western Tianshan, NM China. *Geochimica*, 28(6): 515-520 (in Chinese with English abstract)
- Clemens JD, Holloway JR and White AJR. 1986. Origin of an A-type

- granite: Experimental constraints. *American Mineralogist*, 71(3-4): 317-324
- Coleman RG. 1989. Continental growth of Northwest China. *Tectonics*, 8(3): 621-635
- Collins W, Beams S, White A and Chappell B. 1982. Nature and origin of A-type granites with particular reference to southeastern Australia. *Contributions to Mineralogy and Petrology*, 80(2): 189-200
- Creaser RA, Price RC and Wormald RJ. 1991. A-type granites revisited; assessment of a residual-source model. *Geology*, 19(2): 163-166
- Eby GN. 1990. The A-type granitoids: A review of their occurrence and chemical characteristics and speculations on their petrogenesis. *Lithos*, 26(1-2): 115-134
- Eby GN. 1992. Chemical subdivision of the A-type granitoids: Petrogenetic and tectonic implications. *geology*, 20(7): 641-644
- Frost BR, Barnes CG, Collins WJ, Arculus RJ, Ellis DJ and Frost CD. 2001. A Geochemical Classification for Granitic Rocks. *Journal of Petrology*, 42(11): 2033-2048
- Gao J, He GQ, Li MS, Xiao XX, Tang YQ, Wang J and Zhao M. 1995. The mineralogy, petrology, metamorphic *PTDt* trajectory and exhumation mechanism of blueschists, south Tianshan, northwestern China. *Tectonophysics*, 250(1-3): 151-168
- Gao J, Li MS, Xiao XX, Tang YQ and He GQ. 1998. Paleozoic tectonic evolution of the Tianshan Orogen, northwestern China. *Tectonophysics*, 287(1-4): 213-231
- Gao J, Long LL, Qian Q, Huang DZ, Su W and Klemd R. 2006. South Tianshan: A Late Paleozoic or a Triassic Orogen? *Acta Petrologica Sinica*, 22(5): 1049-1061 (in Chinese with English abstract)
- Gu LX, Hu SX, Yu CS, Li HY, Xiao XJ and Yan ZF. 2000. Carboniferous volcanites in the Bogda orogenic belt of eastern Tianshan: Their tectonic implications. *Acta Petrologica Sinica*, 16(3): 305-316 (in Chinese with English abstract)
- Han BF, He GQ, Wu TR and Li HM. 2004. Zircon U-Pb dating and geochemical features of early paleozoic granites from Tianshan, Xinjiang: Implications for tectonic evolution. *Xinjiang Geology*, 22(1): 4-11 (in Chinese with English abstract)
- Han BF, Wang SG, Jahn BM, Hong DW, Kagami H and Sun YL. 1997. Depleted-mantle source for the Ulungur River A-type granites from North Xinjiang, China: Geochemistry and Nd-Sr isotopic evidence, and implications for Phanerozoic crustal growth. *Chemical Geology*, 138(3-4): 135-159
- Hu AQ, Jahn BM, Zhang GQ, Chen YB and Zhang QF. 2000. Crustal evolution and Phanerozoic crustal growth in northern Xinjiang: Nd isotopic evidence. Part I: Isotopic characterization of basement rocks. *Tectonophysics*, 328(1-2): 15-51
- Hu AQ, Zhang GQ, Chen YB and Zhang QF. 2001. A model of division of the continental crust basement and the time scale of the major geological events in the Xinjiang-based on studies of isotopic geochronology and geochemistry *Xinjiang Geology*, 19(1): 12-19 (in Chinese with English abstract)
- Jahn BM, Wu FY and Chen B. 2000. Granitoids of the Central Asian Orogenic Belt and continental growth in the Phanerozoic. *Transactions of the Royal Society of Edinburgh-Earth Sciences*, 91: 181-193
- Khain EV, Bibikova EV, Salnikova EB, Kroner A, Gibsher AS, Didenko AN, Degtyarev KE and Fedotova AA. 2003. The Palaeo-Asian ocean in the Neoproterozoic and early Palaeozoic: New geochronologic data and palaeotectonic reconstructions. *Precambrian Research*, 122(1-4): 329-358
- King PL, White AJR, Chappell BW and Allen CM. 1997. Characterization and origin of aluminous A-type granites from the Lachlan Fold Belt, Southeastern Australia. *Journal of petrology*, 38(3): 371-391
- Konopelko D, Biske G, Seltmann R, Eklund O and Belyatsky B. 2007. Hercynian post-collisional A-type granites of the Kokshaal Range, Southern Tien Shan, Kyrgyzstan. *Lithos*, 97(1-2): 140-160
- Landenberger B and Collins WJ. 1996. Derivation of A-type granites from a dehydrated charnockitic lower crust: evidence from the Chaelundi Complex, Eastern Australia. *Journal of Petrology*, 37(1): 145-170
- Li HQ, Wang DH, Wan Y, Qu WJ, Zhang B, Lu YF, Mei YP and Zou SL. 2006. Isotopic geochronology study and its significance of the Lailisigao'er Mo deposit, Xinjiang. *Acta Petrologica Sinica*, 22(10): 2437-2443 (in Chinese with English abstract)
- Li XH. 1997. Geochemistry of the Longsheng Ophiolite from the southern margin of Yangtze Craton, SE China. *Geochemical Journal*, 31: 323-37
- Li XH, Qi CS, Liu Y, Liang XR, Tu XL, Xie LW and Yang YH. 2005. Petrogenesis of the Neoproterozoic bimodal volcanic rocks along the western margin of the Yangtze Block: New constraints from Hf isotopes and Fe/Mn ratios. *Chinese Science Bulletin*, 50(21): 2481-2486
- Liu W and Fei PX. 2006. Methane-rich fluid inclusions from ophiolitic dunite and post-collisional mafic-ultramafic intrusion: The mantle dynamics underneath the Palaeo-Asian Ocean through to the post-collisional period. *Earth and Planetary Science Letters*, 242(3-4): 286-301
- Long LL. 2007. Paleozoic tectonic evolution and continental growth of the West Tianshan Orogen: Evidence from granitoids and ophiolites. Beijing: Institute of Geology and Geophysics, Chinese Academy of Sciences, 174
- Ludwig KR. 2003. User's manual for Isoplot 3.00: a geochronological toolkit for Microsoft Excel. Berkeley Geochronology Center Special Publication, 4: 1-70
- Middlemost EAK. 1994. Naming materials in the magma/igneous rock system. *Earth-Science Rev*, 37: 215-224
- Mingram B, Trumbull RB, Littman S and Gerstenberger H. 2000. A petrogenetic study of anorogenic felsic magmatism in the Cretaceous Paresis ring complex, Namibia: Evidence for mixing of crust and mantle-derived components. *Lithos*, 54(1-2): 1-22
- Mushkin A, Navon O, Halicz L, Hartmann G and Stein M. 2003. The Petrogenesis of A-type magmas from the Anram Massif, Southern Israel. *Journal of Petrology* 44(5): 815-832
- Patino Douce AE. 1997. Generation of metaluminous A-type granites by low-pressure melting of calc-alkaline granitoids. *Geology*, 25(8): 743-746
- Pearce JA, Harris NBW and Tindle AG. 1984. Trace element discrimination diagrams for the tectonic interpretation of granitic rocks. *Journal of Petrology* 25(4): 956-983
- Pirajno F, Mao JW, Zhang ZC, Zhang ZH and Chai FM. 2008. The association of mafic-ultramafic intrusions and A-type magmatism in the Tian Shan and Altay orogens, NW China: Implications for geodynamic evolution and potential for the discovery of new ore deposits. *Journal of Asian Earth Sciences*, 32(2-4): 165-183
- Qian Q, Gao J, Klemd R, He GQ, Song B, Liu DY and Xu RH. 2008. Early Paleozoic tectonic evolution of the Chinese South Tianshan Orogen: constraints from SHRIMP zircon U-Pb geochronology and geochemistry of basaltic and dioritic rocks from Xiata, NW China. *International Journal of Earth Sciences*, DOI 10.1007/s00531-007-0268-x
- Qiu JS, Wang DZ and McInnes BIA. 1999. Geochemistry and petrogenesis of the I- and A-type composite granite masses in the central area of Zhejiang and Fujian province. *Acta Petrologica Sinica*, 15(2): 237-246 (in Chinese with English abstract)
- Sengor AMC, Natalin BA and Burtman VS. 1993. Evolution of the Altaid tectonic collage and Palaeozoic crustal growth in Eurasia. *Nature*, 364(6435): 299-307
- Shi YS, Lu HF and Jia D. 1994. Paleozoic plate-tectonic evolution of the Tarim and western Tianshan regions, western China. *International*

- Geology Review, 36(11): 1058–1066
- Sun S and McDonough WF. 1989. Chemical and isotopic systematics of oceanic basalts: Implications for mantle composition and processes. Geological Society London Special Publications, 42(1): 313–345
- Tang GJ, Wang Q, Zhao ZH, Wyman DA, Jiang ZQ and Jia XH. 2008. Geochronology and geochemistry of ore-bearing porphyries in the Lamasu areas, western Tianshan. submitted
- Turner SP, Foden JD and Morrison RS. 1992. Derivation of some A-type magmas by fractionation of basaltic magma: An example from the Padthaway Ridge, South Australia. Lithos, 28(2): 151–179
- Wang B, Faure M, Cluzel D, Shu LS, Charvet J, Meffre S and Qian Ma. 2006a. Late Paleozoic tectonic evolution of the northern West Chinese Tianshan Belt. Geodinamica Acta 19(3–4): 227–237
- Wang B, Shu LS, Cluzel D, Faure M and Charvet J. 2007a. Geochronological and geochemical studies on the Borohoro plutons, north of Yili, NW Tianshan and their Tectonic implication. Acta Petrologica Sinica, 23(8): 1885–1900 (in Chinese with English abstract)
- Wang H and Peng SL. 2000. Determination of volcanicity of ice and its geological significance to Dabate copper ore deposit in wenquan county, Xinjiang. Contributions to Geology and Mineral Resources Research, 15(4): 346–350 (in Chinese with English abstract)
- Wang JB, Wang YW and Wang LJ. 2004a. The Junggar immature continental crust province and its mineralization. Acta Geologica Sinica, 78(2): 337–344 (in Chinese with English abstract)
- Wang JB and Xu X. 2006b. Post-collisional tectonic evolution and metallogenesis in Northern Xinjiang, China. Acta Geologica Sinica, 80(1): 23–31 (in Chinese with English Abstract)
- Wang Q, Wyman DA, Zhao ZH, Xu JF, Bai ZH, Xiong XL, Dai TM, Li CF and Chu ZY. 2007b. Petrogenesis of Carboniferous adakites and Nb-enriched arc basalts in the Alataw area, northern Tianshan Range (western China): Implications for Phanerozoic crustal growth in the Central Asia orogenic belt. Chemical Geology, 236(1–2): 42–64
- Wang Q, Zhao ZH, Xu JF, Wyman DA, Xiong XL, Zi F and Bai ZH. 2006c. Carboniferous adakite-high-Mg andesite-Nb-enriched basaltic rock suites in the Northern Tianshan area: Implications for Phanerozoic crustal growth in the Central Asia Orogenic Belt and Cu-Au mineralization. Acta Petrologica Sinica, 22(1): 11–30 (in Chinese with English abstract)
- Wang ZL, Mao JW, Zhang ZH and Wang LS. 2006d. Geology, time-space distribution and metallogenic geodynamic evolution of porphyry copper (molybdenum) deposits in the Tianshan Mountains Acta Geologica Sinica, 80(7): 943–955 (in Chinese with English Abstract)
- Wang ZL, Mao JW, Zhang ZH and Wang LS. 2004b. Types, characteristics and metallogenic geodynamic evolution of the paleozoic polymetallic copper-gold deposits in the western Tianshan Mountains. Acta Geologica Sinica, 78(6): 836–847 (in Chinese with English Abstract)
- Whalen JB, Currie KL and Chappell BW. 1987. A-type granites: Geochemical characteristics, discrimination and petrogenesis. Contributions to Mineralogy and Petrology, 95(4): 407–419
- Windley BF, Allen MB, Zhang C, Zhao ZY and Wang GR. 1990. Paleozoic accretion and Cenozoic redefinition of the Chinese Tien Shan Range, Central Asia. Geology, 18(2): 128–131
- Wu FY, Sun DY, Li HM, Jahn BM and Wilde S. 2002. A-type granites in northeastern China: Age and geochemical constraints on their petrogenesis. Chemical Geology, 187(1–2): 143–173
- Wu FY, Li XH, Yang JH and Zheng Y, F. 2007. Discussions on the petrogenesis of granites. Acta Petrologica Sinica, 23(6): 1217–38
- Xia LQ, Xia ZC, Xu XY, Li XM and Ma ZP. 2008. Relative contributions of crust and mantle to the generation of the Tianshan Carboniferous rift-related basic lavas, northwestern China. Journal of Asian Earth Sciences, 31(4–6): 357–378
- Xia LQ, Xia ZC, Xu XY, Li XM, Ma ZP and Wang LS. 2004a. Carboniferous Tianshan igneous megaprovince and mantle plume. Geological Bulletin of China, 23(9): 903–910 (in Chinese with English abstract)
- Xia LQ, Xu XY, Xia ZC, Li XM, Ma ZP and Wang LS. 2004b. Petrogenesis of Carboniferous rift-related volcanic rocks in the Tianshan, northwestern China. Geol. Soc. Am. Bull., 116(3–4): 419–433
- Xia LQ, Zhang GW, Xia ZC, Xu XY, Dong YP and Li XM. 2002. Constraints on the timing of opening and closing of the Tianshan Paleozoic oceanic basin: Evidence from Sinian and Carboniferous volcanic rocks. Geological Bulletin of China, 21(2): 55–62 (in Chinese with English abstract)
- Xiao WJ, Han CM, Yuan C, Sun M, Lin SF, Chen HL, Li ZL, Li J and Sun S. 2008. Middle Cambrian to Permian subduction-related accretionary orogenesis of Northern Xinjiang, NW China: Implications for the tectonic evolution of central Asia. Journal of Asian Earth Sciences, 32(2–4): 102–117
- Xiao WJ, Windley BF, Badarch G, Sun S, Li J, Qin K and Wang Z. 2004a. Paleozoic accretionary and convergent tectonics of the southern Altaids: Implications for the growth of Central Asia. Journal of the Geological Society, 161(3): 339–342
- Xiao WJ, Zhang LC, Qin KZ, Sun S and Li JL. 2004b. Paleozoic accretionary and collisional tectonics of the eastern Tianshan (China): Implications for the continental growth of central Asia. American Journal of Science, 304(4): 370
- Xu XY, Li XM, Ma ZP, Xia LQ, Xia ZC and Peng SX. 2006a. LA-ICPMS zircon U-Pb dating of gabbro from the Bayingou Ophiolite in the northern Tianshan Mountains. Acta Geologica Sinica, 80(8): 1168–1176 (in Chinese with English abstract)
- Xu XY, Ma ZP, Xia ZC, Xia LQ, Li XM and Wang LS. 2006b. TIMS U-Pb Isotopic dating and geochemical characteristics of Paleozoic granitic rocks from the middle-western section of Tianshan. Northwestern Geology, 39(1): 50–75 (in Chinese with English abstract)
- Xu XY, Xia LQ, Ma ZP, Wang YB, Xia ZC, Li XM and Wang LS. 2006c. SHRIMP zircon U-Pb geochronology of the plagiogranites from Bayingou ophiolite in North Tianshan Mountains and the petrogenesis of the ophiolite. Acta Petrologica Sinica, 22(1): 83–94 (in Chinese with English abstract)
- Yakubchuk A. 2004. Architecture and mineral deposit settings of the Altaid orogenic collage: A revised model. Journal of Asian Earth Sciences, 23(5): 761–779
- Yang JH, Wu FY, Chung SL, Wilde SA and Chu MF. 2006a. A hybrid origin for the Qianshan A-type granite, northeast China: Geochemical and Sr-Nd-Hf isotopic evidence. Lithos, 89(1–2): 89–106
- Yang SF, Li Z, Chen H, Santosh M, Dong C-W and Yu X. 2007. Permian bimodal dyke of Tarim Basin, NW China: Geochemical characteristics and tectonic implications. Gondwana Research, 12(1–2): 113–120
- Yang SF, Li ZL, Chen HL, Xiao WJ, Yu X, Lin XB and Shi XG. 2006b. Discovery of a Permian quartz syenitic porphyritic dyke from the Tarim basin and its tectonic implications. Acta Petrologica Sinica, 22(5): 1405–1412 (in Chinese with English abstract)
- Yuan HL, Gao S, Liu XM, Li HM, Gunther D and Wu FY. 2004. Accurate U-Pb age and trace element determinations of zircon by laser ablation-inductively coupled plasma mass spectrometry. Geoanalytical and Geostandard Newsletters, 28(3): 353–370
- Zhang LC, Xiao WJ, Qin KZ and Zhang Q. 2006a. The adakite connection of the Tuwu-Yandong copper porphyry belt, eastern Tianshan, NW China: Trace element and Sr-Nd-Pb isotope geochemistry. Mineralium Deposita, 41(2): 188–200

- Zhang LF, Ai YL, Li XP, Rubatto D, Song B, Williams S, Song SG, Ellis D and Liou JG. 2007a. Triassic collision of western Tianshan orogenic belt, China: Evidence from SHRIMP U-Pb dating of zircon from HP/UHP eclogitic rocks. *Lithos*, 96(1-2): 266-280
- Zhang LF, Ai YL, Song SG, Liou J and Wei CJ. 2007b. A brief review of UHP meta-ophiolitic rocks, southwestern Tianshan, western China. *International Geology Review*, 49(9): 811-823
- Zhang ZH, Mao JW, Wang ZL, Du AD, Wang LS, Wang JW and Qu WJ. 2006b. Geology and metallogenetic Epoch of the Dabate porphyry copper deposit in west Tianshan Mountains, Xinjiang. *Geological Review*, 52(5): 683-689 (in Chinese with English abstract)
- Zhu YF, Zhang LF, Gu LB, Guo X and Zhou JB. 2005. The zircon SHRIMP chronology and trace element geochemistry of the Carboniferous volcanic rocks in western Tianshan Mountains. *Chinese Science Bulletin*, 50(19): 2201-2212
- Zhu ZX, Wang KZ, Xu D, Su YL and Wu YM. 2006. SHRIMP U-Pb dating of zircons from Carboniferous intrusive rocks on the active continental margin of Eren Habirga, West Tianshan, Xinjiang, China, and its geological implications. *Geological Bulletin of China*, 25(8): 986-991 (in Chinese with English abstract)

附中文参考文献

- 车自成, 刘洪福, 刘良. 1994. 中天山造山带的形成与演化. 北京: 地质出版社, 135
- 车自成, 刘良. 1996. 论伊犁古裂谷. *岩石学报*, 12(3): 478-490
- 陈义兵, 胡霁琴, 张国新, 张前峰. 1999. 西天山前寒武纪天窗花岗岩片麻岩的锆石 U-Pb 年龄及 Nd-Sr 同位素特征. *地球化学*, 28(6): 515-520
- 高俊, 龙灵利, 钱青, 黄德志, 苏文, KLEMD, R. 2006. 南天山: 晚古生代还是三叠纪碰撞造山带?. *岩石学报*, 22(5): 1049-1061
- 顾连兴, 胡受奚, 于春水, 李宏宇, 肖新建, 严正富. 2000. 东天山博格达造山带石炭纪火山岩及其形成地质环境. *岩石学报*, 16(3): 305-316
- 韩宝福, 何国琦, 吴泰然, 李惠民. 2004. 天山早古生代花岗岩锆石 U-Pb 定年、岩石地球化学特征及其大地构造意义. *新疆地质*, 22(1): 4-11
- 胡霁琴, 张国新, 陈义兵, 张前峰. 2001. 新疆大陆基底分区模式和主要地质事件的划分. *新疆地质*, 19(1): 12-19
- 李华芹, 王登红, 万颀, 屈文俊, 张兵, 路远发, 梅玉萍, 邹绍利. 2006. 新疆莱历斯高尔铜钼矿床的同位素年代学研究. *岩石学报*, 22(10): 2437-2443
- 龙灵利. 2007. 西天山造山带古生代构造演化与地壳增生—来自花岗岩和蛇绿岩的证据. 博士论文. 北京: 中国科学院地质与地球物理研究所, 1-174
- 邱检生, 王德滋, McInnes BIA. 1999. 浙闽沿海地区 I 型-A 型复合花岗岩体的地球化学及成因. *岩石学报*, 15(02): 237-246

- 唐功建, 王强, 赵振华, Wyman, D. A., 姜子琦, 贾小辉. 2008. 西天山喇嘛苏铜矿成矿斑岩的年代学与地球化学特征. 已投稿
- 王博, 舒良树, Cluzel D, Faure M, Charvet J. 2007. 伊犁北部博罗霍努岩体年代学和地球化学研究及其大地构造意义. *岩石学报*, 23(08): 1889-1900
- 王核, 彭省临. 2000. 新疆温泉县达巴特铜矿火山机构的厘定及其意义. *地质找矿论丛*, 15(4): 346-350
- 王京彬, 徐新. 2006. 新疆南部后碰撞构造演化与成矿. *地质学报*, 80(1): 23-31
- 王强, 赵振华, 许继峰, Wyman DA., 熊小林, 资峰, 白正华. 2006. 天山北部石炭纪埃达克岩-高镁安山岩-富 Nb 岛弧玄武质岩: 对中亚造山带显生宙地壳增生与铜金成矿的意义. *岩石学报*, 22(1): 11-30
- 王志良, 毛景文, 张作衡, 左国朝, 王龙生. 2004. 西天山古生代铜金多金属矿床类型、特征及其成矿地球动力学演化. *地质学报*, 78(6): 836-847
- 王志良, 毛景文, 张作衡, 左国朝, 王龙生. 2006. 新疆天山斑岩铜钼矿地质特征、时空分布及其成矿地球动力学演化. *地质学报*, 80(7): 943-955
- 吴福元, 李献华, 杨进辉, 郑永飞. 2007. 花岗岩成因研究的若干问题. *岩石学报*, 23(6): 1217-1238
- 夏林圻, 夏祖春, 徐学义, 李向民, 马中平, 王立社. 2004. 天山石炭纪大火成岩省与地幔柱. *地质通报*, 23(9): 903-910
- 夏林圻, 张国伟, 夏祖春, 徐学义, 董云鹏, 李向民. 2002. 天山古生代洋盆开启、闭合时限的岩石学约束——来自震旦纪、石炭纪火山岩的证据. *地质通报*, 21(2): 55-62
- 徐学义, 李向民, 马中平, 夏林圻, 夏祖春, 彭素霞. 2006a. 北天山巴音沟蛇绿岩形成于早石炭世: 来自辉长岩 LA-ICPMS 锆石 U-Pb 年龄的证据. *地质学报*, 80(8): 1168-1176
- 徐学义, 马中平, 夏祖春, 夏林圻, 李向民, 王立社. 2006c. 天山中西段古生代花岗岩 TIMS 法锆石 U-Pb 同位素定年及岩石地球化学特征研究. *西北地质*, 39(1): 50-75
- 徐学义, 夏林圻, 马中平, 王彦斌, 夏祖春, 李向民, 王立社. 2006b. 北天山巴音沟蛇绿岩斜长花岗岩 SHRIMP 锆石 U-Pb 年龄及蛇绿岩成因研究. *岩石学报*, 22(1): 83-94
- 杨树锋, 厉子龙, 陈汉林, 肖文交, 余星, 林秀斌, 施锡桂. 2006. 塔里木二叠纪石英正长斑岩岩墙的发现及其构造意义. *岩石学报*, 22(5): 1405-1412
- 张作衡, 毛景文, 王志良, 杜安道, 左国朝, 王龙生, 王见隼, 屈文俊. 2006. 新疆西天山达巴特铜矿床地质特征和成矿时代研究. *地质论评*, 52(5): 683-689
- 朱志新, 王克卓, 徐达, 苏延龙, 吴玉门. 2006. 依连哈比尔尕山石炭纪侵入岩锆石 SHRIMP U-Pb 测年及其地质意义. *地质通报*, 25(8): 986-991